

Active Vibration Control for A Bilinear System with Nonlinear Velocity Time-delayed Feedback

X. Gao, Q. Chen

Abstract—The primary resonance, stability and design methodology of a piecewise bilinear system under cubic velocity feedback control with a designed time delay are investigated. Through combining multi-scale perturbation method with Fourier expansion, the effects of time delay on dynamics behaviours are explored. Subsequently, the linearization of average equations obtained from analytical multi-scale method is applied to obtain the corresponding characteristic function, and thus stability boundaries can be determined. In order to obtain the desired vibration control performance, appropriate gain and time delay of feedback are chosen based on the frequency response function and stability conditions. Lastly, the assessment of the influences of the feedback parameters on vibration transmissibility is given. Results show that both feedback gain and time delay are significant factors for altering dynamics behaviours and improving effectiveness of controller.

Index Terms—vibration control, time delay, cubic velocity feedback, piecewise bilinear

I. INTRODUCTION

VIBRATION isolation systems can be divided into three groups: passive, active and semi-active according to external energy requirement. The use of passive isolators is the most common method of controlling undesired vibrations in various engineering sectors such as aerospace engineering, transportation systems, marine engineering, civil engineering etc. [1-3]. The linear viscous damping is often introduced to reduce vibration amplitude at resonance for such a vibration isolation device. Unfortunately, the transmissibility increases with the damping in the frequency region where isolation is required. This is a dilemma that the passive vibration isolation technique faces [4]. But it could be solved by the active or semi-active control method such as direct linear velocity feedback strategy, which is recognized as a simple and robust method. The feedback controller generates an additional force which is proportional to velocity of the equipment, and thus it is sometimes referred to a skyhook damping for it reacts off the structure at required frequencies [5]. The outstanding virtue of on-off skyhook damping is that the resonance peak is reduced without affecting the vibration transmission at higher frequencies [6]. On the other hand,

This work was supported by Natural Science Foundation of China under Grant No. 11272145, Funding of Jiangsu Innovation Program for Graduate Education under grant No. CXLX12_0135 and the Fundamental Research Funds for the Central Universities.

Corresponding author Q. Chen is with Nanjing University of Aeronautics and Astronautics (NUAA), Nanjing, 210016 China (phone: +86-25-84893221; fax: +86-25-84893221; e-mail: q.chen@nuaa.edu.cn).

First author X. Gao is with NUAA (e-mail: xgao.detec@nuaa.edu.cn).

conventional skyhook unfortunately introduces a sharp increase (jump or jerk often called in papers) in damping force, which, in turn, causes a jump in sprung-mass acceleration [7-9]. In order to figure out the dilemma of the design of passive linear damped vibration isolation and eliminate the acceleration jump induced by the sudden change of damping force, the present paper proposes an active controller of cubic velocity time-delayed feedback. By comparison with a passive device, the active controller is a practical approach to provide an exact cubic damping force as demanded. Besides, the feedback gain of the control strategy is fixed, not displacement- or velocity-dependent and consequently dynamics jerk induced by the sudden change of damping force could be avoided.

But in real active control system, one of open problems is the complicated system dynamics induced by the unavoidable time delay in controllers and actuators, especially in various analogue filters. The downsides of the time delay on the stability and performance of a dynamics system has drawn a great deal of attention from researchers in structural dynamics engineering [10-14]. However, if designed properly, the time delay existed in controller could suppress bifurcations and improve vibration control [15,16]. This paper is to explore the dynamics of a bilinear vibration control system with cubic velocity time delay feedback and propose a proper design methodology for the controller.

II. MULTI-SCALE ANALYSIS

A. Frequency response

Fig. 1 shows a single degree-of-freedom vibration system with an active vibration controller. Actually, the passive model of nonlinear stiffness and linear damping are abstracted from a solid and liquid mixture vibration (SALiM) isolator [17].

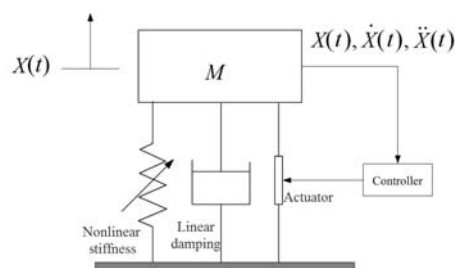


Fig. 1 The active control system

The equation of motion of a bilinear vibration control system with cubic velocity feedback can be represented by

$$M\ddot{X}(t) + C_1\dot{X}(t) + C_2\dot{X}^3(t - \delta) + F_k[X(t)] = F \cos \omega t \quad (1)$$

where M , C_1 , $F \cos \omega t$ are mass, linear viscous damping coefficient and excitation force respectively. C_2 and δ denote the feedback gain and time delay involved in the control loop. The restoring force can be described by piecewise linear function with respect to the displacement, as

$$F_k(X) = \begin{cases} K_1 X & (X \geq a_c) \\ K_2 X + (K_1 - K_2)a_c & (X < a_c) \end{cases} \quad (2)$$

where a_c is the coordinate value of discontinuity point on displacement axis, and K_1, K_2 are stiffness coefficients.

Using the following dimensionless system parameters

$$\omega_0 = \sqrt{\frac{K_1}{M}}, \Omega = \frac{\omega}{\omega_0}, T = \omega_0 t, \tau = \omega_0 \delta, X = x a_c,$$

$$\xi_1 = \frac{C_1}{2M\omega_0}, \xi_2 = \frac{C_2(a_c\omega_0)^3}{K_1 a_c}, f = \frac{F}{K_1 a_c}$$

one can easily obtain

$$\frac{dX(t)}{dt} = \omega_0 a_c \frac{dx(T)}{dT}, \quad \frac{d^2 X(t)}{dt^2} = \omega_0^2 a_c \frac{d^2 x(T)}{dT^2},$$

$$\frac{dX(t - \delta)}{dt} = \omega_0 a_c \frac{dx(T - \tau)}{dT}.$$

Substituting those transformations into (2) yields dimensionless equation of motion

$$\ddot{x}(T) + x(T) + 2\xi_1\dot{x}(T) + \xi_2\dot{x}^3(T - \tau) + \varepsilon g[x(T)] = f \cos \Omega T \quad (3)$$

where dot denotes differentiation with respect to T , and the nonlinearity factor is defined as

$$\varepsilon \stackrel{\text{def}}{=} 1 - \frac{K_2}{K_1}, \quad (4)$$

and

$$g(x) = \begin{cases} 0 & (x \geq 1) \\ -(x - 1) & (x < 1) \end{cases} \quad (5)$$

To analyze the primary resonance of the system with time delay control given in Eq.(3) by using the multi-scale perturbation method combined with Fourier expansion, one confines the study to the case of small damping, weak nonlinearity, weak feedback and low level excitation [14], i.e.

$$\xi_1 = \varepsilon \hat{\xi}_1, \quad \xi_2 = \varepsilon \hat{\xi}_2, \quad f = \varepsilon \hat{f}, \quad \Omega^2 = 1 + \varepsilon \sigma, \quad \sigma = O(1).$$

$$\ddot{x}(T) + x(T) = \varepsilon \{-g[x(T)] - 2\hat{\xi}_1\dot{x}(T) - \hat{\xi}_2\dot{x}^3(T - \tau) + \hat{f} \cos \Omega T\} \quad (6)$$

For simplicity, first order approximate with two time scales is introduced herein $x(T) = x_0(T_0, T_1) + \varepsilon x_1(T_0, T_1) + O(\varepsilon^2)$, $T_r = \varepsilon^r T$, $r = 0, 1$. Using following differential operators and substituting them into (6),

$$\begin{cases} \frac{d}{dT} = \frac{\partial}{\partial T_0} + \varepsilon \frac{\partial}{\partial T_1} + O(\varepsilon^2) \equiv D_0 + \varepsilon D_1 + O(\varepsilon^2) \\ \frac{d^2}{dT^2} = D_0^2 + 2\varepsilon D_0 D_1 + O(\varepsilon^2) \end{cases} \quad (7)$$

then equating the same power of ε produce

$$\varepsilon^0: D_0^2 x_0(T_0, T_1) + \Omega^2 x_0(T_0, T_1) = 0 \quad (8)$$

$$D_0^2 x_1(T_0, T_1) + \Omega^2 x_1(T_0, T_1)$$

$$\varepsilon^1: = -2D_0 D_1 x_0(T_0, T_1) - g[x_0(T_0, T_1)] - 2\hat{\xi}_1 \dot{x}_0(T_0, T_1) - \hat{\xi}_2 \dot{x}_0^3(T_0 - \tau, T_1) + \hat{f} \cos \Omega \tau + \sigma x_0(T_0, T_1) \quad (9)$$

The solution of Eq. (8) is

$$x_0(T_0, T_1) = a(T_1) \cos[\Omega T_0 + \varphi(T_1)] \quad (10)$$

Substituting (10) into (9) yields

$$\begin{aligned} D_0^2 x_1(T_0, T_1) + \Omega^2 x_1(T_0, T_1) &= -2(-\Omega D_1 a \sin \phi - \Omega a D_1 \varphi \cos \phi) - g[x_0(T_0, T_1)] \\ &+ (\hat{f} \cos \phi \cos \varphi + \hat{f} \sin \phi \sin \varphi) \\ &+ 2\hat{\xi}_1 \Omega a \sin \phi - \hat{\xi}_2 (-a\Omega)^3 \sin^3(\phi - \Omega \tau) + \sigma a \cos \phi \end{aligned} \quad (11)$$

where $\phi = \Omega T_0 + \varphi(T_1)$. In order to eliminating secular term in (11), the coefficients of basic harmonics $\sin \phi$ and $\cos \phi$ must be zero, i.e.

$$2\Omega D_1 a + \hat{f} \sin \varphi + 2\hat{\xi}_1 \Omega a + \frac{3}{4} \hat{\xi}_2 a^3 \Omega^3 \cos(\Omega \tau) + A_1 = 0 \quad (12)$$

$$2\Omega a D_1 \varphi + \hat{f} \cos \varphi + \sigma a - \frac{3}{4} \hat{\xi}_2 a^3 \Omega^3 \sin(\Omega \tau) + A_2 = 0 \quad (13)$$

where A_1 and A_2 are the coefficients of basic harmonics of Fourier series of term $-g(x_0)$. As can be seen in (5), $g(x_0)$ is a piecewise linear function, thus the integral can be calculated in three intervals: $[0, \varphi_0]$, $[\varphi_0, 2\pi - \varphi_0]$ and $[2\pi - \varphi_0, 2\pi]$, where φ_0 corresponds to the phase of discontinuity point in a vibration cycle.

Then $D_1 a$ and $D_1 \varphi$ are obtained from (12) and (13) as follows

$$D_1 a = -\frac{1}{2\Omega} [\hat{f} \sin \varphi + 2\hat{\xi}_1 \Omega a + \frac{3}{4} \hat{\xi}_2 a^3 \Omega^3 \cos(\Omega \tau)] \quad (14)$$

$$a D_1 \varphi = -\frac{1}{2\Omega} [\hat{f} \cos \varphi + \sigma a - \frac{3}{4} \hat{\xi}_2 a^3 \Omega^3 \sin(\Omega \tau) + A_2] \quad (15)$$

For a steady primary resonance, $D_1 a = D_1 \varphi = 0$. Then the application of $(\sin \varphi)^2 + (\cos \varphi)^2 = 1$ gives

$$[2\hat{\xi}_1 \Omega a + \frac{3}{4} \hat{\xi}_2 a^3 \Omega^3 \cos(\Omega \tau)]^2 \quad (16)$$

$$+ [(\Omega^2 - 1)a - \frac{3}{4} \hat{\xi}_2 a^3 \Omega^3 \sin(\Omega \tau) + \varepsilon A_2]^2 = f^2$$

To verify the reliability of perturbation method, the nonlinear frequency response is also constructed by a fourth order Runge-Kutta scheme in association with a stepped-sine excitation and FFT technique. Fig. 2 compares the analytic displacement response and that from above stepped-sine simulation. There is an excellent agreement between analytical results and numerical references, especially in cases of $\tau = 0$ and $\tau = \frac{\pi}{4}$. And what is most

interesting is that a separate closed-loop of solution branch emerges above primary curve in Fig.2(c). But numerical simulation is not capable of producing the corresponding data. Similarly in Fig. 2(d), one still cannot obtain numerical data in the frequency band confined between vertical broken lines. In fact, the cause that those solution branches cannot be estimated by numerical integration is the instability, and this conclusion will be supported by stability analysis in the next section.

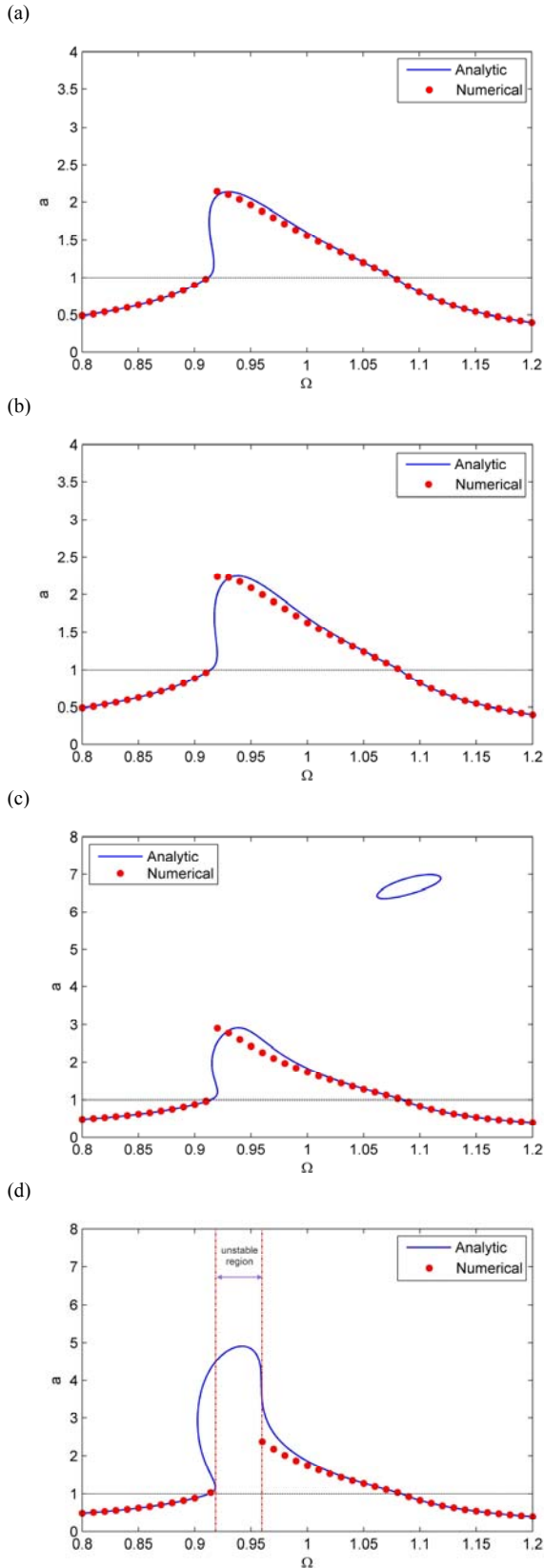


Fig. 2 Displacement frequency response of systems with different time delays ($\xi_1=0.03$, $\xi_2=0.01$, $\varepsilon=0.6$, $f=0.1786$): (a) $\tau = 0$, (b) $\tau = \frac{\pi}{4}$, (c) $\tau = \frac{2\pi}{4}$, (d) $\tau = \frac{3\pi}{4}$.

In fact, the additional closed-loop response curve in Fig.2(c) is due to multiple solution branches satisfying extremum condition of $\frac{da}{d\Omega} = 0$ in [18]. As can be seen from

Fig. 2(c), there are three solution branches over the frequency band covering the frequency island. If two or three of branches are stable, a sudden jump could occur in the sine-sweep test.

B. Stability boundary

To analyse the stability of steady state primary resonance, linearizing Eqs. (14) and (15) with respect to φ and a yields

$$D_1 \Delta a = -[\hat{\xi}_1 + \frac{9}{8} \hat{\xi}_2 a^2 \Omega^2 \cos(\Omega \tau)] \Delta a + \frac{1}{2\Omega} [\sigma a - \frac{3}{4} \hat{\xi}_2 a^3 \Omega^3 \sin(\Omega \tau) + A_2] \Delta \varphi \quad (17)$$

$$D_1 \Delta \varphi = \frac{1}{a} [-\frac{1}{2\Omega} \sigma - \frac{1}{2\Omega} A_2' + \frac{9}{8} \hat{\xi}_2 a^2 \Omega^2 \sin(\Omega \tau)] \Delta a - \frac{1}{2\Omega a} [2\hat{\xi}_1 \Omega a + \frac{3}{4} \hat{\xi}_2 a^3 \Omega^3 \cos(\Omega \tau)] \Delta \varphi \quad (18)$$

Further, the characteristic equation of Eqs. (17) and (18) is

$$\lambda^2 + [2\hat{\xi}_1 + \frac{3}{2} \hat{\xi}_2 a^2 \Omega^2 \cos(\Omega \tau)] \lambda + S_1 S_4 - S_2 S_3 = 0 \quad (19)$$

where, S_1, S_2, S_3, S_4, A_2 and A_2' are not given for brevity.

From the Routh–Hurwitz criterion, the steady-state vibration is asymptotically stable if and only if the following two inequalities hold simultaneously

$$\Sigma_1 \stackrel{\text{def}}{=} 2\hat{\xi}_1 + \frac{3}{2} \hat{\xi}_2 a^2 \Omega^2 \cos(\Omega \tau) > 0 \quad (20)$$

and

$$\Sigma_2 \stackrel{\text{def}}{=} S_1 S_4 - S_2 S_3 > 0 \quad (21)$$

As a matter of fact, if condition Eq.(20) stands up but inequality (21) does not hold, the response is unstable due to the occurrence of saddle-node bifurcation, which means that the jump phenomenon could happen. If $\Sigma_1 < 0$, the dynamics response of vibration system will diverge despite Eq.(21) holds or not. Actually, the stability boundary $\Sigma_1 = 0$ indicates the critical condition that the sign of real parts of both roots of characteristic equation changes. A change from negative real parts to positive real parts indicates the presence of a supercritical Hopf bifurcation [12]. For the uncontrolled system only with the positive damping, $\Sigma_1 = 2\hat{\xi}_1 > 0$, and hence Hopf bifurcation is excluded.

Fig. 3 shows the unstable regions of primary resonance responses for systems with different time delays. The parts of curves covered by shaded regions represent unstable solutions.

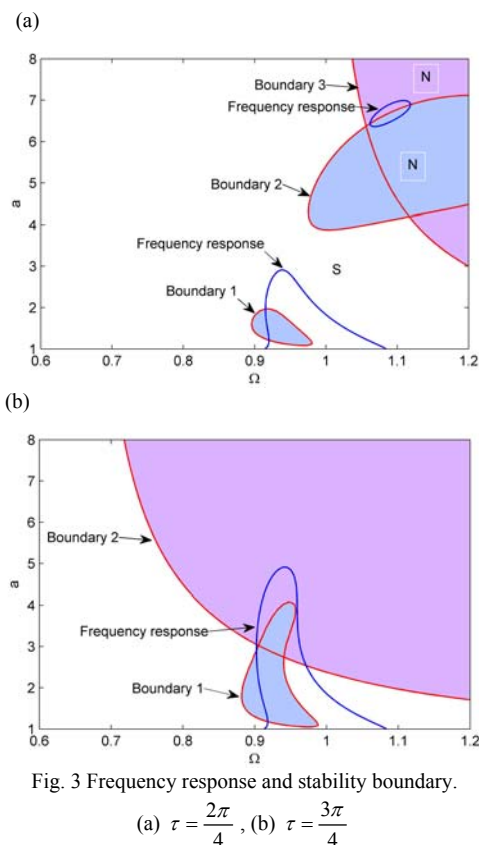


Fig. 3 Frequency response and stability boundary.

(a) $\tau = \frac{2\pi}{4}$, (b) $\tau = \frac{3\pi}{4}$

In the case of time delay $\tau = \frac{2\pi}{4}$, both stability boundaries 1 and 2 are obtained from Eq.(21) and boundary 3 is given by Eq.(20). It is obvious that the entire closed curve solution is covered by a shaded unstable region confined by the boundary 3. For the system with time delay $\tau = \frac{3\pi}{4}$, Eqs.(21) and (20) produce stability boundaries 1 and 2 respectively, and the upper of the frequency response curve is cut off by boundary 2. As a matter of fact, those unstable solutions cannot be obtained by numerical simulation. Thus the missing parts of the frequency responses curve in Fig.2 can be illustrated in this way.

III. SELECTION OF FEEDBACK PARAMETERS (ξ_2, τ)

Based on the preceding work, one is ready to do quantitative analysis on how the feedback parameters (time delay and gain) affect the vibration level from the view of vibration control. Since the nonlinear system behaviours can be influenced by the controller's feedback parameters, one can manipulates the dynamic response of the nonlinear system by forcing the selected time delay and feedback gain of the controller. This will be the task of nonlinear system vibration control with cubic velocity feedback and time delay.

Fig.4 shows the influence of time delay τ on the vibration amplitude for a given system. The solid line determined by Eq.(20) depicts the variation of amplitude as time delay increases, and the broken line indicates stability boundary Σ_1 . Compared with controlled system with time delay ($\tau \neq 0$), the controlled system without time delay ($\tau = 0$) can produce lower displacement amplitude. On the

other hand, from the comparison between Fig.4 (a) and (b), it is clear that the stronger feedback gain ξ_2 brings down the vibration amplitude, but shrinks the stable region. In the case of $\xi_2 = 0.1$ (Fig. 4(b)), some parts of the responses are rounded up in unstable regions leading to unstable responses.

Hp1, Hp2 Hp3 and Hp4 indicate the positions where the Hopf bifurcation occurs, and the solid lines between Hp1-Hp2 and Hp3-Hp4 are unstable response branches. For example, the time response as $\tau = 1.0$ is a steady state vibration (see Fig. 5(a)), and on the contrast, the response as $\tau = 3.0$ which is between Hp1 and Hp2 is divergent, as shown in Fig.5(b). The numerical results are obtained by the four-order Runge-Kutta method.

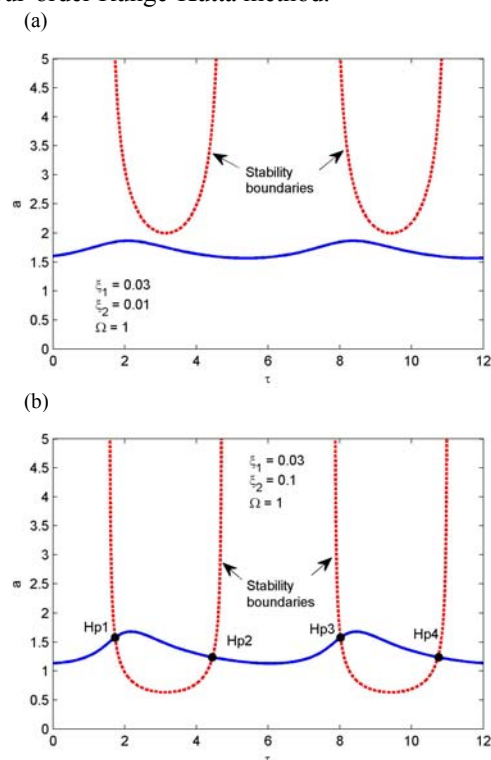


Fig. 4 For a system with different gains, effect of time delay on vibration amplitude and stability boundary Σ_1 .

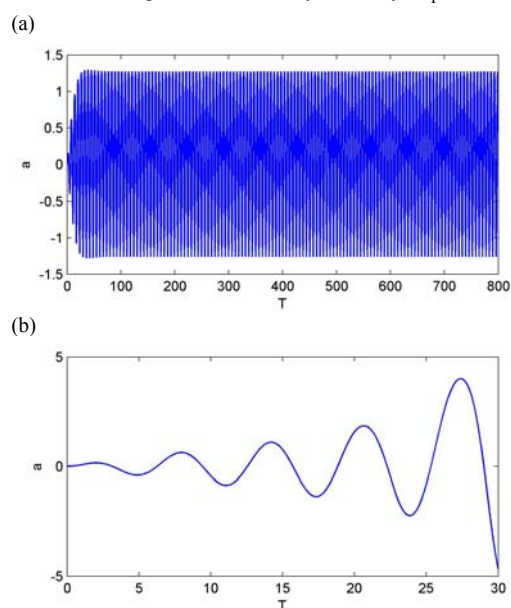


Fig. 5 Numerical time response: (a) $\tau = 1.0$; (b) $\tau = 3.0$.

For a vibration control system, the maximum displacement amplitude is usually suppressed under a target level. Since the maximum displacement depends on the feedback parameters, how to choose gain ξ_2 and feedback time delay τ will be expatiated by an example. Given the system with parameters ($f=0.1786$; $\varepsilon=0.6$, $\Omega=1$), the design procedure is to aim the control target of the dimensionless amplitude limit $a_d < 1.2$. Firstly, it is straightforward to determine the division line in parameter plane (ξ_2, τ) like those in Fig.6 using the frequency response Eq.(20). In Fig.6, the dashdotted, broken and solid lines represent the division of $a_d=1.2$ corresponding to dimensionless linear damping coefficients $\xi_1=0.03, 0.05$ and 0.07 . The whole plane is divided into two parts by the division line, and on the upper plane, the displacement amplitude governed by parameter pair (ξ_2, τ) is less than the specified limit value. Unfortunately, not all parameter pairs located in the upper part satisfy the stability conditions. Hence, it is necessary to identify the corresponding stability boundaries as shown in Fig. 6, which could exclude those feedback parameters falling in the unstable region. As shown in the figure, the solid lines respectively with triangle square and circle are three stability boundaries related to linear damping coefficient $\xi_1=0.03, 0.05$ and 0.07 , and the regions encircled by stability curves represent inappropriate parameter pairs.

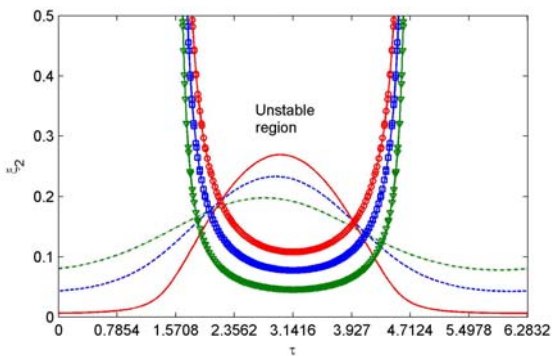


Fig. 6. Design illustration of feedback gain and time delay (dash-dotted, broken and solid lines correspond to the case of $\xi_1=0.03, 0.05$ and 0.07 respectively. Solid lines with triangle, square and circle are corresponding stability boundaries determined by Eq.(39))

IV. SOME SIMPLE ILLUSTRATIONS ON TRANSMISSIBILITY

Once the desired control feedback is determined, it is a straightforward step to evaluate the effectiveness of vibration control system, and the performance characteristics of the control system are dependent on four parameters: nonlinearity factor ε , nondimensional linear damping ratio ξ_1 , nondimensional nonlinear damping ratio ξ_2 and nondimensional time delay τ . The theme of following discussion focuses on influence of ξ_1, ξ_2 and τ on vibration isolation performance, i.e. force transmissibility T_f which is determined by the ratio of maximum output force to maximum excitation force. The Runge-Kutta algorithm is employed again to estimate force transmissibility and how the force transmissibility changes with system parameters. The results are given in Fig. 7-9.

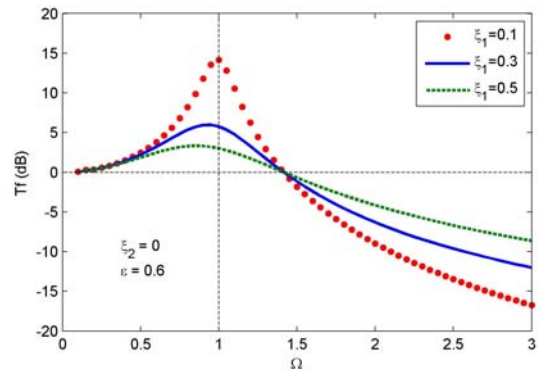


Fig. 7 Effect of linear damping on vibration transmissibility for the uncontrolled system.

Fig. 7 shows the variation of transmissibility as the linear damping coefficient increases. As one might expect, the increase of linear damping reduces the transmissibility peak and consequently suppress the vibration in resonance region. However, the dilemma occurs that the increase of ξ_1 is detrimental for vibration control in frequency band where isolation is required.

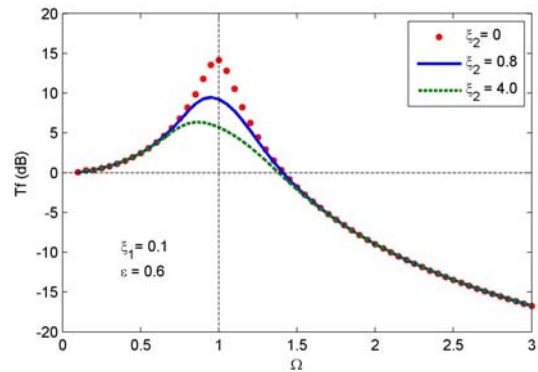


Fig. 8 Effect of cubic nonlinear damping on force transmissibility for controlled systems.

For controlled system without time delay, Fig. 8 compares the effect of feedback gain on the force transmissibility between three cases of $\xi_2 = 0, 0.8$ and 4.0 . It is manifest that the increase of feedback gain can not only reduce transmissibility and suppress vibration in resonance region but keep them unchanged over higher frequency range. Therefore, cubic velocity feedback breaks through the barrier existing in the passive vibration control system with linear damping.

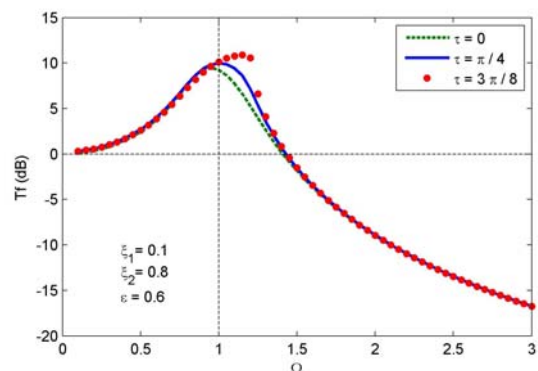


Fig. 9 Effect of time delay on vibration transmissibility for controlled systems.

When time delay is considered, the situation becomes a little different and more complicated, as shown in Fig. 9. As be seen, the resonance peak shifts towards to higher

frequency direction as the time delay increases. And what is worse is that transmissibility peak rises.

In fact, there are two interesting cases of systems in terms of response property: the first is that the maximum amplitude is below the critical displacement point, i.e. $a < 1$. In this case, the adverse influence of time delay on transmissibility peak has been shown in Fig. 9 and thus the control scheme with very small time delay is preferable to control vibration. The results illustrated in Figs.7 and 8 correspond to the case as well. The second is that the break point is crossed, i.e. $a \geq 1$, and the vibrating system exhibits softening stiffness property. On this condition, the time delay might exhibit its favorable effect on the vibration transmissibility. In Fig.10, the dot line shows the emergence of jump phenomenon induced by the piecewise linear stiffness. As can be seen interestingly, the jump disappears as time delay increases and transmissibility peaks are almost same.

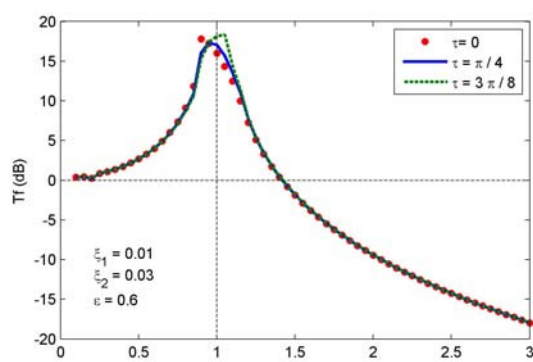


Fig. 10 Effect of time delay on vibration transmissibility for controlled systems in case of $a \geq 1$

V. CONCLUSIONS

In this article, a controlled vibration system with piecewise linear stiffness and cubic velocity feedback has been considered from aspects of its primary resonance analysis, concept design of feedback parameters and vibration transmissibility. Several conclusions are summarized as follows:

- 1) The frequency response of the system has been found analytically by utilizing the multi-scale method. It has been shown that the multi-scale analysis works well the time-delayed controlled system with piecewise linear stiffness described in Figure 1. The accuracy of solution was limited to time delay involved in the feedback loop.
- 2) To control the vibration level below a specified value, the two feedback parameters are examined on the frequency response and stability boundaries which must be complied to exclude the feedback parameter values that might cause unstable system behaviour.
- 3) It is found that the gain can not only reduce the whole force transmissibility level and greatly suppress vibration in region resonance, but also can keep the transmissibility unchanged over higher frequency range where vibration isolation is required.
- 4) The jump phenomenon in sine-sweep test could be avoided by appropriate time delay, as can be seen in Fig.10.

- 5) Meanwhile the jerks induced by sudden change of damping force in conventional skyhook can be avoided due to the smoothly imposed control force.

REFERENCES

- [1] S. N. Mahmoodi, M. Ahmadian. "Modified acceleration feedback for active vibration control of aerospace structures." *Smart material and structure*, vol. 19, no. 6, 065015(10pp), 2010.
- [2] Q. Hu, G. Ma. "Variable structure control and active vibration suppression of flexible spacecraft during attitude maneuver," *Aerospace Science and Technology*, vol. 9, no. 4, pp. 307-317, 2005
- [3] H. Ma, G. Y. Tang, Y. D. Zhao. "Feedforward and feedback optimal control for offshore structures subjected to irregular wave forces," *Journal of Sound and Vibration*, vol. 33, no. 8-9, pp. 1105-1117, 2006
- [4] Z. Q. Lang, X. J. Jing, S. A. Billings, et al. "Theoretical study of the effects of nonlinear viscous damping on vibration isolation of sdf systems," *Journal of Sound and Vibration*, vol. 323, no. 1-2, pp. 352-365, 2009
- [5] S. J. Elliott, M. Serrano and P. Gardonio. "Feedback stability limits for active isolation system with reactive and inertial actuators," *Journal of Vibration and Acoustics*, vol. 123, no. 2, pp. 250-261, 2001
- [6] S. R. Will, M. R. Kidner, B. S. Cazzolato, et al. "Theoretical design parameters for a quasi-zero stiffness magnetic spring for vibration isolation," *Journal of Sound and Vibration*, vol. 326, no. 1-2, pp. 88-103, 2009.
- [7] Y. Liu, T. P. Waters, M. J. Brennan. "A comparison of semi-active damping control strategies for vibration isolation of harmonic disturbances," *Journal of Sound and Vibration*, vol. 280, no. 1-2, pp. 21-39, 2005.
- [8] M. Ahmadian, X. Song, S. C. Southward. "No-Jerk skyhook control methods for semiactive Suspensions," *Journal of Vibration and Acoustic*, vol. 126, no. 4, pp. 580-584, 2004
- [9] Y. M. Wang. "Research on characteristics of on-off control for semi-active suspensions of vehicle," *Chinese Journal of Mechanical Engineering*, vol. 38, no. 6, pp. 148-151, 2002
- [10] M. S. Ali, Z. K. Hou, M. N. Noori. "Stability and performance of feedback control systems with time delays," *Computers and Structures*, vol. 66, no. 2-3, pp. 241-248, 1998
- [11] A. Maccari. "Vibration control for the primary resonance of the van der Pol oscillator by a time delay state feedback," *International Journal of Non-Linear Mechanics*, vol. 38, no. 1, pp. 123-131, 2003
- [12] A. Maccari. "The response of a parametrically excited Van der Pol oscillator to a time delay state feedback," *Nonlinear Dynamics*, vol. 26, no. 2, pp. 105-119, 2001
- [13] N. Eslaminasab, M. F. Golnaraghi. "The effect of time delay of the semi-active dampers of on-off control schemes," *ASME 2007 International Mechanical Engineering Congress and Exposition*, Seattle, USA, 2007,
- [14] H. Hu, E. H. Dowell, L. N. Virgin. "Resonances of a harmonically forced Duffing oscillator with time delay state feedback," *Nonlinear Dynamics*, vol. 15, no. 4, pp. 311-327, 1998.
- [15] Y. Zhao, J. Xu. Mechanism analysis of delayed nonlinear vibration absorber, *Chinese Journal of theoretical and applied mechanics*, vol. 40, no. 1, pp. 98-106, 2008
- [16] Nayfeh N, Baumann W. "Nonlinear analysis of time-delay position feedback control of container cranes," *Nonlinear dynamics*, vol. 53, no. 1, pp. 75-88, 2008
- [17] X. Gao, Q. Chen and H. D. Teng. "Modelling and dynamics properties of a novel solid and liquid mixture vibration isolator," *Journal of Sound and Vibration*, vol. 331, no. 16, pp.3695-3709, 2012
- [18] A. Narimani, M. F. Golnaraghi, G. N. Jazar. "Sensitivity Analysis of the Frequency Response of a Piecewise Linear System in a Frequency Island," *Journal of Vibration and Control*, vol. 10, no. 2, pp. 175-198, 2004